

Functionalised graphene effect on the mechanical and thermal properties of recycled PA6/PA6,6 blends

Journal of Composite Materials
2021, Vol. 55(16) 2211–2224
© The Author(s) 2021



Article reuse guidelines:
sagepub.com/journals-permissions
DOI: 10.1177/0021998320987897
journals.sagepub.com/home/jcm



Feras Korkees¹ , Abdullah Aldrees¹, Imad Barsoum² and Dalal Alshammari¹

Abstract

Limiting the generation of polymers waste and maximizing their recyclability and recovery have been the main focus of the research and industry in recent years. Recycling of polyamides leads to the loss in mechanical and thermal properties, therefore, in order to reuse recycled nylons, an enhancement in their properties is desired. Enhancing the properties of recycled polyamides by the addition of functionalised graphene nanoparticles (GNPs) was the goal of this study. Recycled PA6/PA6,6 blends and functionalised graphene nanocomposites were prepared using hot-melt extrusion process. Two types of functionalised graphene were used: O₂-GNPs and Amine-GNPs. The nanofillers didn't affect the crystallinity of the recycled nylon, while the presence of functionalised graphene increased the thermal conductivity by enabling better heat transfer routes within the polymer. The microstructure of the materials was characterised confirming the successful dispersion but with a slight variation in GNPs/Polymer bonding depending on the functionalisation type. The strong nylon-to-graphene interfacial hydrogen bonding increased the mechanical properties of the recycled nylon nanocomposites. The functionalised nanoparticles slowed down the segmental motion of the polymer chain and decreased the ductility with increasing GNPs contents up to 10 wt%. The overall behaviour of recycled nylon nanocomposites showed dependency on the type of functionalisation and concentration of GNPs with better improvement in the overall properties using 2 wt% Amine-GNPs. These enhanced properties make functionalised graphene/recycled nylon nanocomposites a promising new class of advanced materials.

Keywords

Nanocomposites, polyamide, mechanical properties, thermal properties, polymer blends

Introduction

In the recent years, polymer–nanoparticle composite materials have attracted research and commercial interest due to their unique mechanical, electrical, optical and thermal properties. Developments in nanocomposites are rapidly advancing and the possibility of producing materials with enhanced properties using graphene nano-platelets (GNPs) is particularly of interest.

Thermoplastic materials are of interest in industry due to their low cost and ease of processing and recyclability, in addition to other properties such as rigidity and high impact strength.^{1–5} Polyamide is a semi-crystalline polymer with low density, excellent wear and chemical resistance, alongside excellent strength, hardness and impact properties.⁶ Polyamides have been used in various applications for nearly 80 years,

and their sector is expected to grow over 6.1% from 2017 to 2025 since polyamide can be easily modified to specific requirements in a wider range of applications.^{6–8} Plastics degrade very slowly over hundreds of years, and one of the biggest problems today is the waste produced annually by their use and the long-lasting effects it has on the environment.⁹ Therefore, taking use of the whole polymer's life-span is crucial.^{10,11} Researches have been focusing on limiting

¹Materials Research Centre, Swansea University, UK

²Khalifa University of Science and Technology, UAE

Corresponding author:

Feras Korkees, Materials Research Centre, College of Engineering, Swansea University, Swansea SA1 8EN, Wales, UK.

Email: f.a.korkees@swansea.ac.uk

the plastic waste generation, with the aim to reduce the use of resources and maximize recovery.⁶ Since mechanical properties change when products made of nylons are recycled, it is important to know whether recycled nylon is something that could be used in products that need high mechanical strength or is it a hopeless case.^{12,13} Numerous researches have been carried out on improving the properties of recycled thermoplastics and specifically PAs by either blending it with other polymers^{14–20} or by adding multi-scale reinforcement materials.^{21–34} However, as to knowledge, no previous studies have attempted to enhance the mechanical properties of recycled polyamides and polyamide blends by incorporating functionalised graphene.

Graphene has attracted great attention because of its unique two-dimensional (2D) structure and novel properties. What makes graphene even more interesting is that it only requires a small amount to be incorporated into the polymer to enhance its properties and this is due to its high surface area. Several studies reported challenges in manufacturing nanocomposites such as achieving uniform dispersion, as well as good interfacial adhesion between components. Modification of graphene is achieved by adding functional groups to the surface or edge of graphene nanoplatelets through covalent bonding and non-covalent bonding.¹³ The functionalisation of graphene is crucial because it determines the quality of the dispersion and bonding of nanoparticles and polymers. The effect of unfunctionalized graphene and carbon-nanotubes on the properties of PA6, PA6,6 and other polymers has been studied. An increase in crystallinity of these polymers by the presence of nanoparticles was reported^{35–37} but also a reduction in crystallinity was seen by other researchers.^{38–40} The addition of nanoparticles into polymers was also seen to improve their thermal conductivity which depends on the interfacial bonding between the polymer chains and the reinforcement phase.^{41–47} Xu B et al.⁴⁵ investigated the effect of graphene on PA6/PA6,6 blend and their results showed that the thermal conductivity of PA6/PA6,6 blend increased 10 times when 50 wt% GNPs were added. Previous work on assessing the shore hardness of polymer composites reported slight increase which was attributed to the high surface area and dispersion of the reinforcement phase.^{48–50} Incorporating GNPs in polymeric materials have been seen to lead to an increase^{35,51,52} and reduction^{45,53–55} in tensile properties. Yesildag et al.⁵² reported a 20% increase in tensile modulus when 1 wt% GNPs was added to PA6. The researchers claimed that further increase in graphene content does not significantly increase the modulus due to possible agglomeration. Keledi et al.⁵⁴ proposed that the materials strength is highly dependent on the strength of nanoparticles/polymer

interface. With regard to the flexural properties of PAs, an improvement has been reported by some researchers.^{45,56} Xu et al.⁴⁵ observed slight improvement in the flexural modulus of PA6/PA6,6 blend with increasing GNPs content up to 50%. On the other hand, the flexural strength decreased by 2 MPa when 50% GNPs were added to the PA6/PA6,6 blend.

In this study, the effect of O₂ and Amine functionalised graphene on the properties of recycled PA6/PA6,6 blend has been investigated. The work stems from a novel plasma-treatment process that can produce functionalised multi-layer graphene particles. The study hoped that suitable choice of these groups could improve the dispersion and bonding of the graphene in polymers, leading to improved properties.

Materials and samples preparation

Recycled PA6/PA6,6 blend (4MID 23B20000 ABK200-4Plas) provided by Perpetuus carbon Technology in the form of pellets was used in this study. Both types of functionalised graphene (O₂ – GNPs and Amine – GNPs) used in this study were provided by Perpetuus Carbon Technologies Ltd with surface area of 500 m²/g. The functional groups attached covalently to the O₂-GNPs are generally carbonyls (C=O), alcohols (-OH), and carboxylic acids (COOH). These functional groups allow for hydrogen bonding with other hydroxyl groups, hydrogen atoms, and other molecules. Amine-GNPs contains the amine functional group which consists of basic nitrogen atom which are able to hydrogen bond with other functional groups. Graphene stacks developed by Perpetuus and used in this study can be seen in the SEM images in Figure 1. The green-bluish area shows a dense population of graphenes less than three atomic layers, the green area shows three atomic layers, and the red dot shows a small zone populated at about twenty atomic layers.

A melt mixing method was used to incorporate the functionalised graphene in the polymers. Figure 2 shows the schematic diagram, profile and configuration of 10-mm twin-screw compounder/extruder made by (Rondol Technology Ltd., UK). The screw elements can be classified by their functions into two major groups: conveying/feed elements and mixing blocks. Screws diameter is 10 mm and their Length/Diameter ratio is 20:1. The processing temperature, rotation speeds are given in Table 1. The low extrusion process temperature is because the extruded strand is sensitive to the temperature-dependent viscosity. Therefore, to have good control on the extruded strand when pulling it through the water and into the pelletizer, the temperature had to be lower than melting temperature so the viscosity will be high enough to allow consistency in pulling the strand.

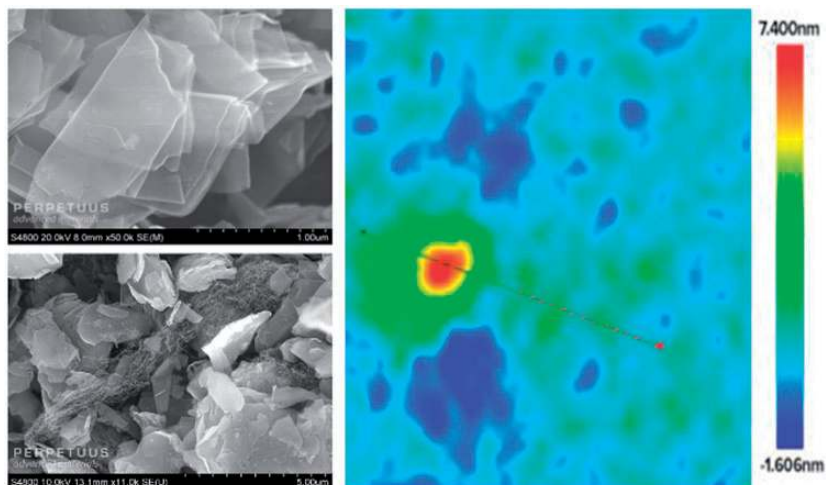


Figure 1. SEM images of Perpetuus Graphene stacks.

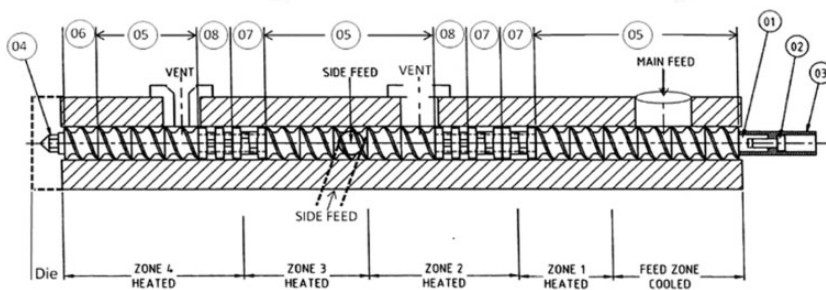


Figure 2. Configuration and profile of the twin-screw extruder: 01(Hex Shaft), 02 (Coupling retaining screw), 03 (Coupling), 04 (Screw tip), 05 (Feed screw), 06 (Extrusion screw), 07 (4 × 60° Mixing/Kneading blocks), and 08 (4 × 90° Mixing/Kneading blocks).

Table 1. Settings of the twin screw extruder.

Material	Temperature setting of the extruder zones (°C)	Screw speed (rpm)	Pellets feeder speed (rpm)	Powder feeder speed	Pelletizer (m/min)
PA6 Blend/GNPs	228/232/245/210/120	90	9	31	2

The pellet and powder feeders were calibrated before mixing to give the rates (g/min) needed to produce a 10 wt% masterbatch. The 10 wt% masterbatch was subsequently diluted to various GNPs concentrations, Table 2.

Test specimens were shaped using a Moore Hydraulic compression moulder. The material was pre-heated in the moulder at 280°C for 10 mins by closing the platens enough to make contact with the mould faces but without any pressure applied. Once the conditions were stable and the material was melted, the platens were closed and pressed at 3 tons for 2 mins followed by cooling to room temperature.

Testing

Shore hardness

Shore Hardness was measured using shore durometer type D scales (ISO 7619/ASTM D2240). These tests used three disks moulded according to EN ISO 868:2003 and BS 2782-3 Method 365B:1981, Figure 3.

Tensile and flexural tests

Five dog-bone samples moulded according to BS ISO 37:2011 – type 2 were used for the tensile tests, while

for the flexural test, five rectangular samples moulded according to BS EN ISO 178:2010 + A1:2013 were used, Figure 3. A Hounsfield electro-mechanical test machine was used for both testing with a load-cell of 25 KN. Tests were performed at two different speeds with 0.5 mm/min in the first stage up to 0.3% elongation followed by speed of 5 mm/min until failure. An Epsilon E97197 extensometer (3542-025 M-010-ST) was used to measure the strain. Modulus values from the tensile tests were estimated from the slope of the

stress/strain curve as close as possible to the strain interval between $\varepsilon_1 = 0.05\%$ and $\varepsilon_2 = 0.25\%$.

Differential scanning calorimetry

A PerkinElmer (8000) DSC was used to measure the crystallinity of the GNPs/nylon blends composites. Two samples of each type were tested with samples weight between 15–20 mg. The DSC analysis was performed in a nitrogen atmosphere with a flow rate of 20 mL/min. The samples were heated from 30°C to 300°C at a heating rate of 10°C/min. After it is kept at an isothermal state for 3 min, the temperature was ramped from 300°C to 30°C at cooling rate of 30°C/min.

The apex of the peak was taken as the melting point. Polymer crystallinity was determined with DSC by quantifying the heat associated with melting (fusion) of the polymer, Figure 7. This heat is reported as Percent Crystallinity by normalizing the observed heat of fusion to that of a 100% crystalline sample of the same polymer. The degree of crystallinity was calculated according to equation (1).

$$\text{Crystallinity \%} = \frac{\Delta H_m}{\Delta H_m^{\text{ideal}}} \times 100 \quad (1)$$

where ΔH_m is the measured heat of fusion, and $\Delta H_m^{\text{ideal}}$ is the melting enthalpy of 100% crystalline PA6 and PA6,6, which is assumed to be 230.1 (J/g) and 255.8 (J/g), respectively.²⁵

Thermal conductivity measurement

Thermal conductivity was measured using a LaserComp Fox 50 instrument. This measures the heat flux between two plates with a specified

Table 2. List of prepared Graphene/PA6/PA6,6 blends composites with varying GNPs content.

Sample	PA6/PA6,6 blend, g (wt%)	GNPs, g (wt%)
PA6/PA6,6 + GNPs-0 %	100.00	0.00
PA6/PA6,6 + GNPs-0.1%	99.90	0.10
PA6/PA6,6 + GNPs-0.5%	99.50	0.50
PA6/PA6,6 + GNPs-1.0%	99.00	1.00
PA6/PA6,6 + GNPs-2.0%	98.00	2.00
PA6/PA6,6 + GNPs-5.0%	95.00	5.00
PA6/PA6,6 + GNPs-10.0%	90.00	10.00



Figure 3. Illustrations of samples types.

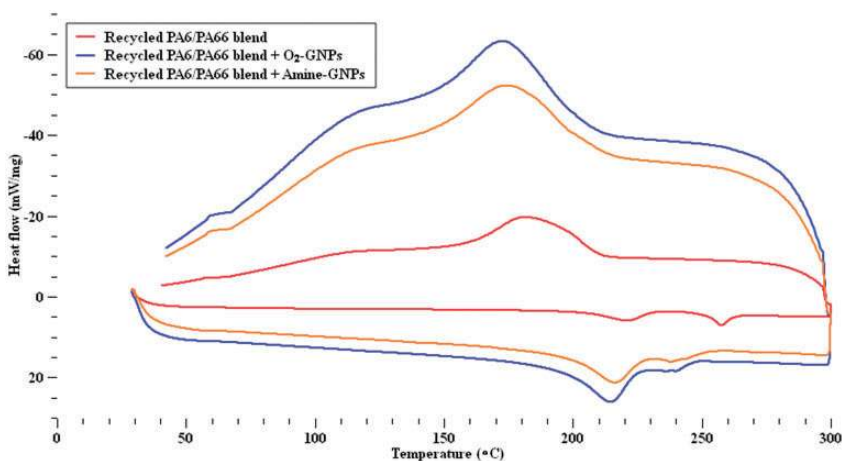


Figure 4. DSC curves of the unfilled and filled recycled PA6/PA66 blend.

temperature differential, in this case between 33°C and 13°C. These tests used disc samples 60 mm in diameter and 6 mm thick. Three sample of each type was used, Figure 3.

Microscopy

The main aim here was to investigate the dispersion and bonding of the nano particles into the polymer. A freeze fracture technique was used to make samples for microscopy tests. The samples were immersed in liquid nitrogen (−196°C) for 1–2 hours and then freeze fractured on a plane through the sample to reveal the internal structure on the nanocomposites. This is to inspect the dispersion and bonding of the GNPs in the matrix. The fractured bit of the samples was loaded on stubs using silver paint. Samples were then coated with platinum to avoid charging on the SEM. A Hitachi Ultra-High-Resolution FE-SEM S-4800 system was used to take the images.

Results and discussion

Differential scanning calorimetry

DSC test results of the recycled PA6/PA6,6 blend, Figure 4, showed two melting peaks one around 220°C (PA6) and one at 257°C (PA6,6). It can be observed that the melting temperatures have shifted slightly to lower temperatures for both PA6 and PA6,6 with the addition of both types of GNPs. The melting point values of both PA6 and PA6,6 in the blend for all composites are given in Table 3. Table 3 shows that the incorporation of Amine-GNPs to the blend decreased the melting temperatures of PA6 and PA6,6 in the blend to 215°C–220°C and 237°C–256°C respectively compared to 221°C and 357°C for

the pure recycled nylon blend. It can observe from Figure 4 that there is one crystallisation peak for the PA6/PA6,6 blend. This can be due to the reason that PA6,6 component crystallizes first forming long, separate lamellae which, at a lower temperature, serve as nucleation substrates for PA6.¹⁸ On the other hand, the addition of O₂-GNPs to the blend dropped the melting temperatures of PA6 and PA6,6 in the blend to 214°C–219°C and 241°C–250°C respectively which are relatively similar to those ranges of Amine-GNPs composites. The reduction in melting temperatures can be explained by possible miscibility in the two materials leading to crystal defects and degradation.^{18,57} Moreover, the crystallisation temperatures of the nanocomposites were slightly lower than that of pure recycled nylon blend, which can be attributed to the promotion of pseudo-hexagonal (λ) phase' nucleation by the graphene nanoparticles.^{16–18} It can also be attributed to the heterogeneous nucleation induced by the graphene nanosheets acting as nucleating agents during the crystallization of the nylon blend.⁵⁸

The crystallinity of PA6 and PA6,6 in the blend before and after the addition of O₂ and Amine GNPs was obtained by determining their melting enthalpies by measuring the area of their melting peaks. The enthalpy values were then compared with a library value for 100% crystalline PA6 and PA6,6 using equation (1) to give an estimate of the crystallinity. The enthalpy and crystallinity values of PA6 and PA6,6 are given in Table 3. Although no significant changes in the degree of crystallinity observed in the nanocomposites, the addition of both types of functionalised graphene yielded some fluctuation on the degree of crystallinity. Figure 5 shows that the addition of O₂-GNPs to the blend slightly increased the crystallinity of both PA6 and PA6,6 at 0.1% content followed by

Table 3. DSC characterization of recycled PA6/PA6,6 samples.

Sample	Melt peak temperature (°C)		Enthalpy (J/g)		Crystallinity (%)	
	PA6	PA6,6	PA6	PA6,6	PA6	PA6,6
PA6/PA6,6 + GNPs-0 %	221	257	18.3	7.6	8	3
PA6/PA6,6 + NH2 GNPs-0.1%	215	237	22.4	2.9	10	1
PA6/PA6,6 + NH2 GNPs-0.5%	218	254	19.8	5.2	9	2
PA6/PA6,6 + NH2 GNPs-1.0%	220	256	26.7	13.5	12	5
PA6/PA6,6 + NH2 GNPs-2.0%	219	256	24.3	9.7	11	4
PA6/PA6,6 + NH2 GNPs-5.0%	221	256	23.5	9.5	10	4
PA6/PA6,6 + NH2 GNPs-10.0%	216	238	20.7	7.6	9	3
PA6/PA6,6 + O2 GNPs-0.1%	219	250	31.3	13	14	5
PA6/PA6,6 + O2 GNPs-0.5%	215	241	22.2	2.8	10	1
PA6/PA6,6 + O2 GNPs-1.0%	216	245	21.1	5	9	2
PA6/PA6,6 + O2 GNPs-2.0%	216	247	22.4	4.8	10	2
PA6/PA6,6 + O2 GNPs-5.0%	217	243	24.8	3	11	1
PA6/PA6,6 + O2 GNPs-10.0%	214	240	24.6	2	11	1

gradual decrease with the increasing of the GNPs content in the blend. On the other hand, the crystallinity of PA6 and PA6,6 reached their highest values at 1% when Amine-GNPs were added to the blend. That was followed by gradual reduction in crystallinity as the GNPs content increased. The reduction in crystallinity can be caused by nanoparticles stacks that prevent polymer chains partially to arrange into crystalline phase.⁵⁸ However, the crystallinity of PA6 and PA6,6 didn't change significantly with the incorporation of O₂ and Amine GNPs. Both types of GNPs tended to increase and decrease the crystallinity of the recycled PA6 and PA6,6 at different concentrations with no clear dependency on the type of functionalisation. The results found are close to other results found in

the literature, claiming that large presence of the GNPs blocks the formation of ordered crystalline phases at high GNPs percentages.^{36,38} It can also be mentioned that the slight increase in crystallinity at low GNPs content might be due more effective sites provided by GNPs for the polymer to nucleate and grow.

Shore hardness

The results obtained from the hardness test shows an increase trend when GNPs content increased as shown in Figure 6. Addition of graphene slightly increased the shore hardness of the pure unreinforced polymer by 5% and 3% at 10% content of Amine-GNPs and O₂-GNPs, respectively. This agrees with previous work

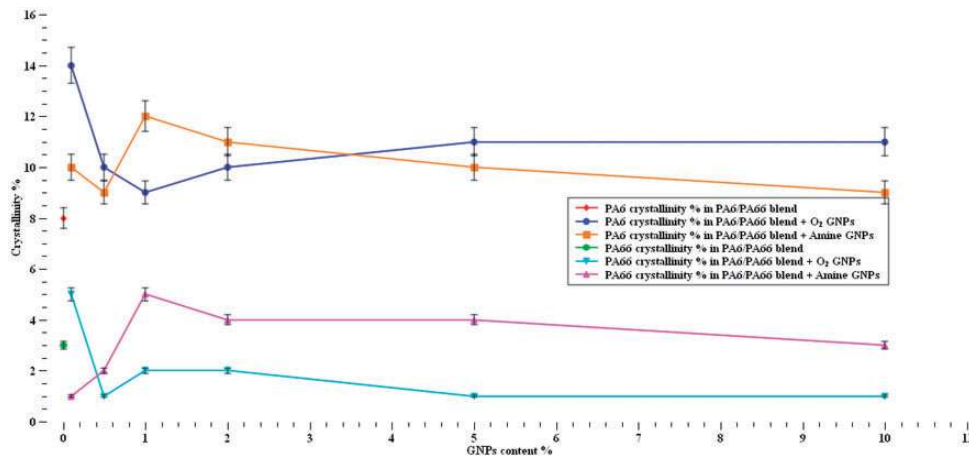


Figure 5. Crystallinity of recycled PA6/PA66 blend with and without GNPs.

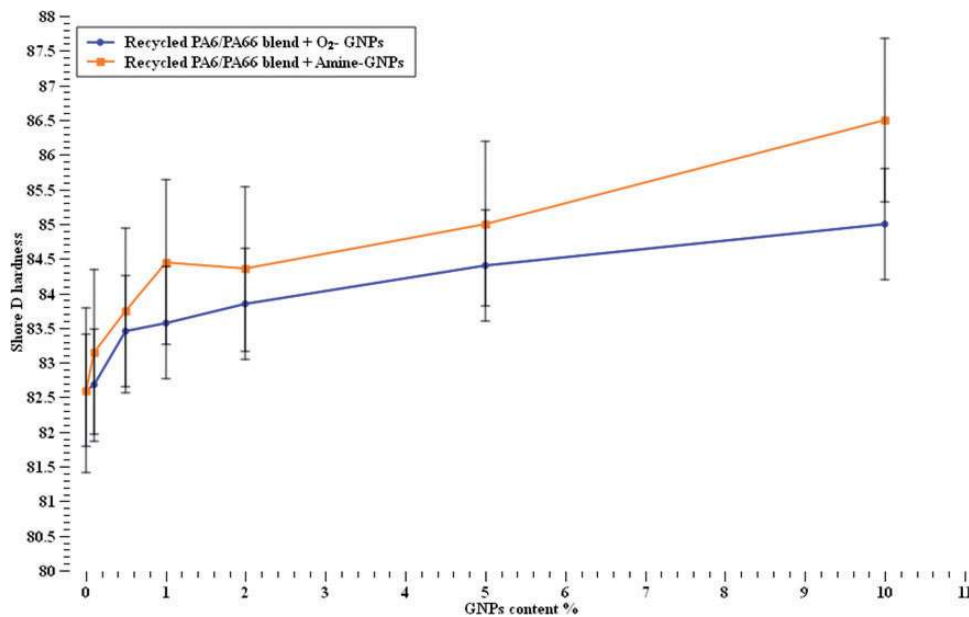


Figure 6. Shore hardness values of recycled PA6/PA66 blend with and without nanofillers.

carried out which showed an increase in hardness values due to the high surface area and hardness properties that GNPs and generally carbon based nano-material possess.⁴⁷⁻⁴⁹ This phenomenon arises from the increment in the incorporation of functionalised GNPs, which is denser and harder than recycled PA6/PA6,6 blend.⁵⁸ The increase trend observed in the shore hardness with increasing both types of GNPs content also indicates that the surface of the nanocomposites become more homogeneous and harder. The increase in shore hardness can also be due to the flexibility of the GNPs in the polymer matrix as explained by La et al.⁵⁰ Amine-GNPs is seen to be more effective with the recycled nylon blend when compared to the O2 functionalisation. This suggests a dependency on the type of functionalisation. This can be attributed to the chemical compatibility and covalent/hydrogen interactions between

Amine groups on the GNPs surface and N-H groups on the nylon structure.

Tensile properties

The results of maximum strength from the tensile tests are shown in Figure 7. It can be observed that the tensile strength increased with increasing Amine-GNPs contents up to 2% while the strength decreased with GNPs content of 5% and higher. On the contrary, a slight variation in the strength at various concentrations was seen with O2-GNPs/recycled nylon blend samples. This small variation is aligned with the literature on assessing the strength of polymer-based nano-composites.^{45,51,53} The increase in strength with Amine-GNPs can be attributed to the effective stress transfer via functionalisation, which provided better interfacial strength and thus withstanding higher

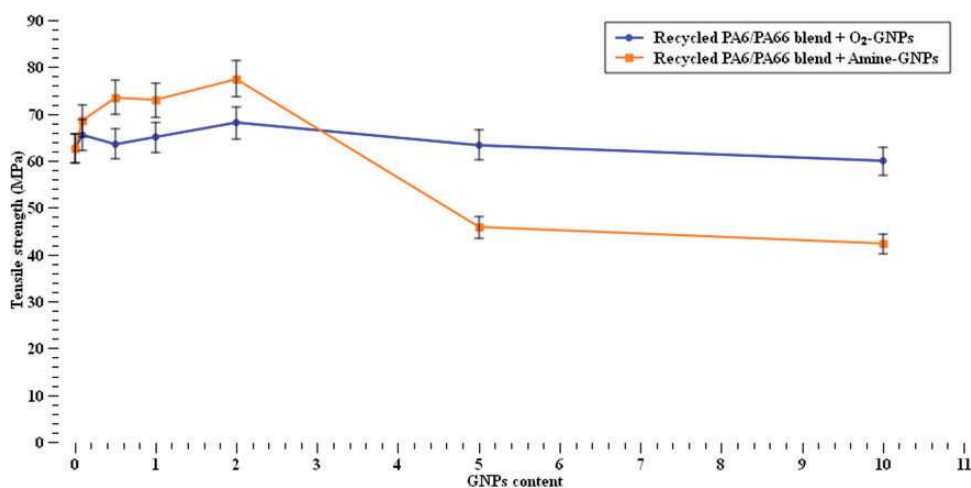


Figure 7. Tensile strength at different GNPs concentrations.

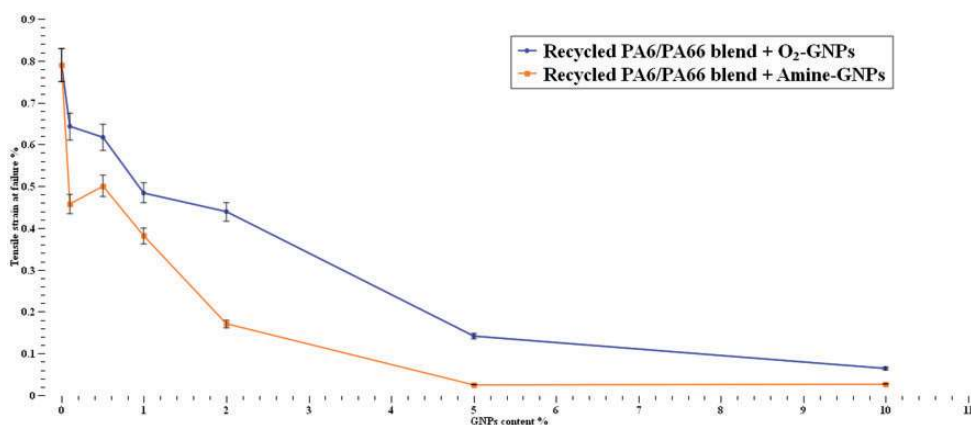


Figure 8. Tensile strain at failure at various GNPs content.

loads compared to O₂-GNPs.⁵⁴ However, the increase in GNPs addition percentage is believed to reduce the strength of the polymer because of their large volume and surface area, leading to an overall reduction in strength. To the authors knowledge no report has yet shown considerable improvements in the mechanical properties of recycled PA polymers at such low concentration as those seen here.

The strain to failure results in Figure 8 show that the ductility of the polymer reduced significantly with increasing GNPs content for both types of GNPs. Addition of graphene to the recycled nylon blend reduced the ductility of the polymer by 20%–40% at 0.1% GNPs content and further reduction at higher concentrations. The incorporation of O₂-GNP shows slightly better results than those of Amine-GNPs. This trend complies with the literature.^{53–55,60} Since carbon materials are inherently brittle, this reduction can be attributed to the presence of rigid and brittle 2-D phase GNPs which can lead to restriction in the polymer chain movement.⁵⁵ Another explanation is that graphene nanoparticles or any other nano-reinforcement can act as stress concentration sites leading to failure without prior ductility.

The modulus of virgin recycled nylon blend is seen to increase between 5%–50% with increasing Amine-GNPs concentration, Figure 9. For O₂-GNPs/recycled nylon blend samples, the modulus decreased initially at low GNPs content up to 1% followed by a slight increase up to 10%. There is no robust reason for this behaviour, but this can be due to the effect of GNPs orientation, which is usually not known.⁵⁴ The modulus values follow trends found in the literature in regard to the effect of GNPs on thermoplastic materials.^{35,51,52} When Amine and O₂ functionalisation are compared, it becomes evident that Amine functionalisation is more effective. This proves that the type of surface modification does affect the stiffness of the material since it contributes to the interfacial strength. This does not comply though with Yesildag,⁵² where it was found that the interfacial strength has no effect on the stiffness of PA6/graphene composites. Furthermore, it can be added that the high surface area of the GNPs increased the interfacial bonding between the GNPs and the nylons matrix resulting in good stress transfer from the polymer matrix to the GNPs nanoparticles which in turn led to improvement in tensile strength and modulus.

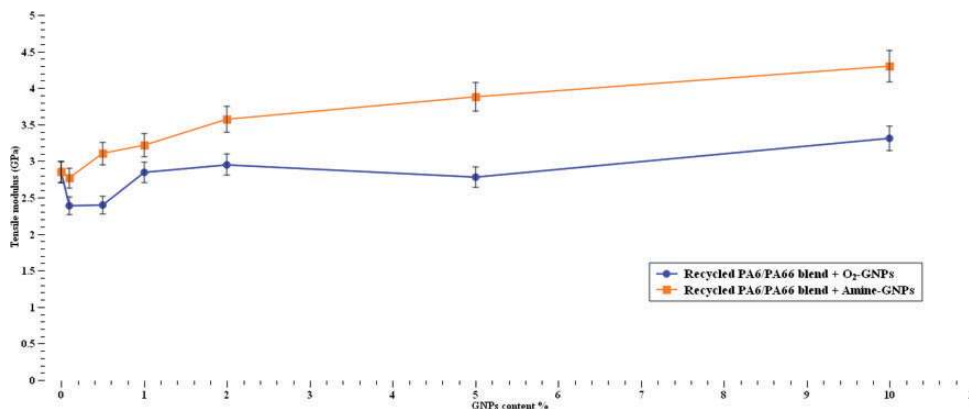


Figure 9. Tensile stiffness at different GNPs concentrations.

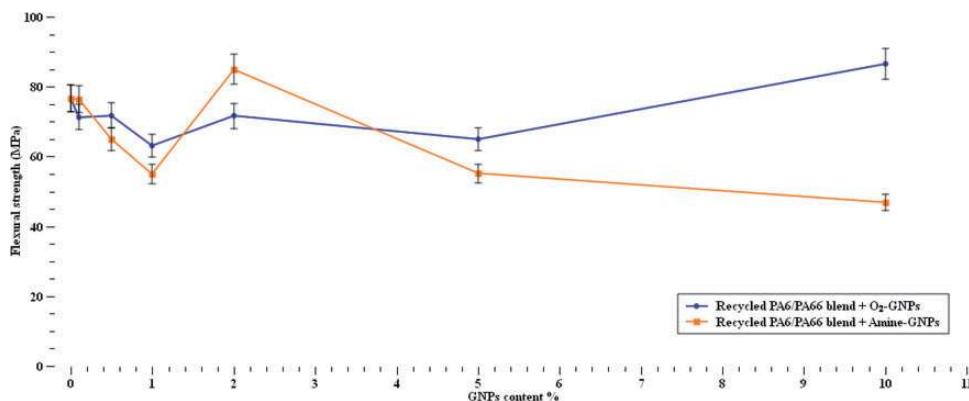


Figure 10. Flexural strength at different GNPs contents.

Flexural properties

When a bending force was applied, the flexural strength of the recycled nylon blend, Figure 10, varied in the presence of both types of GNPs at most of the concentration s. Up to 40% drop in flexural strength was observed with Amine-GNPs samples with one exception at 2% GNPs content where the strength increased by 11%. This behaviour can be due to achieving an optimum number of GNPs that allow effective load transfer and enabling bending of the polymer chains or to the effect of the GNPs orientations.⁵⁴ O₂-GNPs were also found to decrease the flexural strength at concentration s up to 5% but the strength started to increase at 10% GNPs content with 13% enhancement. The odd increase at 10% O₂-GNPs content might be associated with sufficient interfacial bonding at some sites in the microstructure. The results

obtained are in a good agreement with those reported in the literature.^{45,56}

Figure 11 shows that Amine-GNPs have a significant influence on the strain to failure of recycled nylons blend. The ductility of the recycled nylon blend fluctuated with the increase of amine-GNPs content with the maximum reduction of 80% found at 10% of GNPs content. On the other hand, a variation in the flexural strain values of O₂-GNPs/recycled nylon blend composites were noticed with an increase at 0.5% and 5% GNPs contents. This reduction can be due to the presence of the rigid GNPs which in turn led to restriction in the polymer chain movement. The fluctuation can also be attributed to the effect of the GNPs orientations.⁵⁴

Furthermore, Figure 12 shows that increasing the concentration of Amine-functionalised graphene significantly increased the flexural stiffness up to 102% at

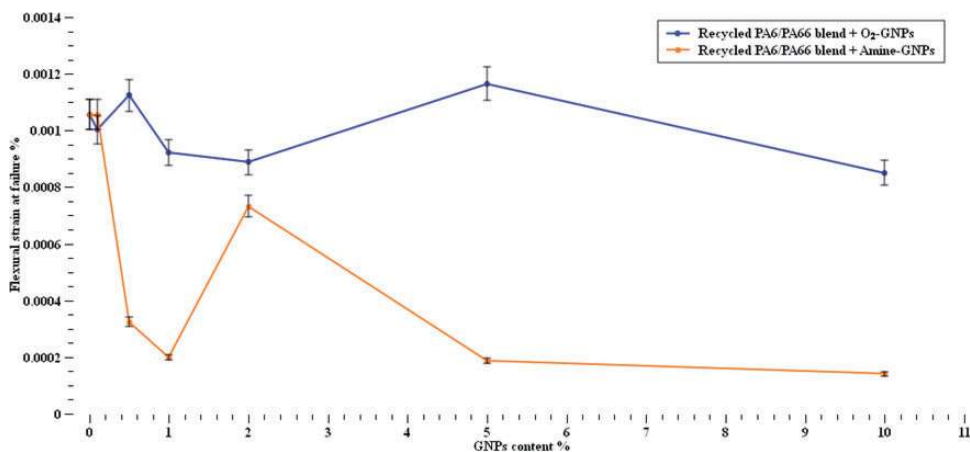


Figure 11. Flexural strain at failure at various GNPs concentrations.

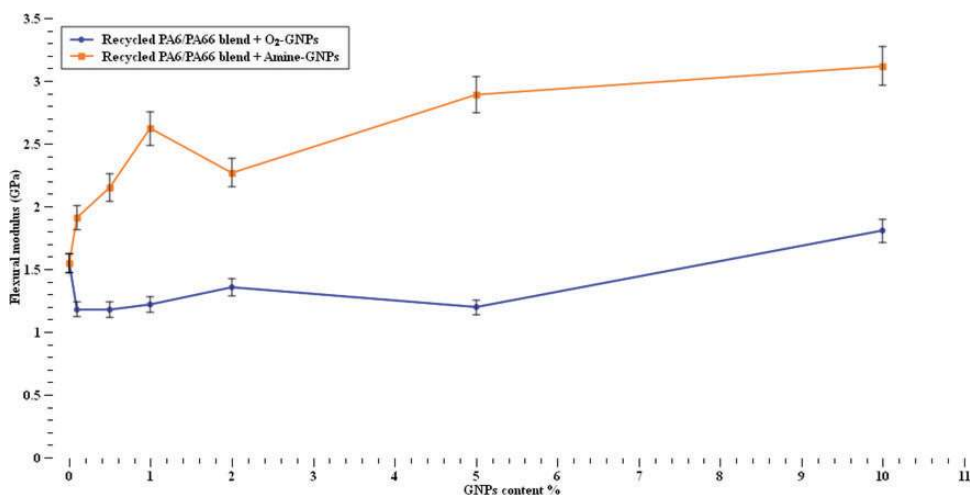


Figure 12. Flexural stiffness at different GNPs contents.

10% Amine-GNPs content. On the other hand, increasing O₂-GNPs up to 5% GNPs concentration reduced the flexural stiffness but slight increases in modulus noted at 10% content. The graph illustrates that the functionalization type has a significant effect on how the polymer flexural modulus behaves. The results found aligned with work found in the literature.^{45,56,60} The Amine functionalisation shows its superiority by probably providing stronger Hydrogen bonding and thus allowing better load transfer and showing a higher impact on the material's flexural modulus. The O₂-GNPs exhibited minor effect, with most values being less than the unloaded polymer, apart from 10% where a slight increase was observed. This can be related to the reduction in strain where the segmental motion of polymer chains is slower due to the restriction imposed by the nanoparticles. The enhancements in the flexural properties of Amine-graphene/recycled nylon blend nanocomposites could probably be attributed to the excellent mechanical properties presented by the functionalised graphene and their high surface area. Since strength, modulus and strain at failure exhibited a complex behaviour, this suggests that the existence of functionalised graphene affected the fracture process of the composites, even at very low contents of GNPs.

Thermal conductivity

The thermal conductivity values for the studied materials are shown in Figure 13. The addition of graphene would be expected to increase thermal conductivity and those results do support the expectations. Thermal conductivity of the recycled nylon blend increased with increasing the GNPs content up to 26% for O₂-GNPs and 59% for Amine-GNPs at 10% content. Therefore, it can be said that Amine-GNPs enabled heat transfer routes within the polymer chains by creating interlayers more efficiently than the O₂-GNPs. The graph illustrates a dependency on the type of

functionalisation since Amine-GNPs showed elevated thermal conductivity compared with O₂-GNPs. The gradual increase in thermal conductivity with increasing the functionalised GNPs concentration agrees with results from⁴²⁻⁴⁵ and no percolation threshold is noticed. Since both types of GNPs showed significant increase in thermal conductivity, therefore it is safe to say that surface modification of the graphene is an efficient method to improve graphene-polymer interface interaction. This also agrees with other studies that surface modification can enhance the interfacial force between graphene and polymer and also the GNPs dispersion in the polymer.¹³ It was reported that thermal conductivity of the recycled nylon blend was improved by 56.9% by the addition of 10% GO-graphene.¹³ Additionally, it can be said that the effective distribution of the functionalised GNPs had its impact on the formation of thermal networks around the specimens' area, which resulted in improvement in thermal conductivity using both types of functionalised graphenes.

Microscopy

A number of SEM images were taken to inspect the dispersion and bonding nature of the functionalised GNPs into the recycled nylon blend. It can be seen from the micrographs in Figure 14 that the O₂- and Amine- GNPs are well dispersed and the particles are well distributed with no agglomeration observed. This suggests that good dispersion can be achieved using functionalised nanoparticles and a reasonable shear mixing by the twin screws. The functional groups (O₂ and Amine) attached to the graphenes surface proved their capability to break that strong van der Waal forces between carbon nanoparticles which is responsible for agglomeration and thus improved GNPs dispersion in the matrix.

The images in Figure 15 show the interfacial bonding between the host matrix and the surface modified functionalised graphene. The images show a strong

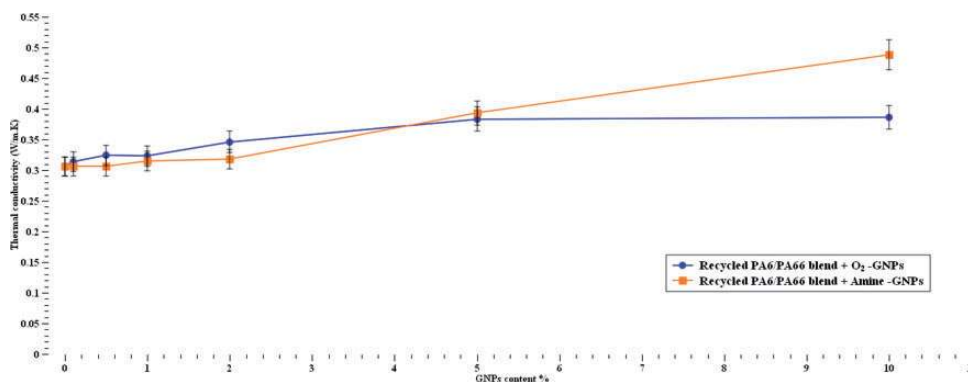


Figure 13. Thermal conductivity as a function of different GNPs contents.

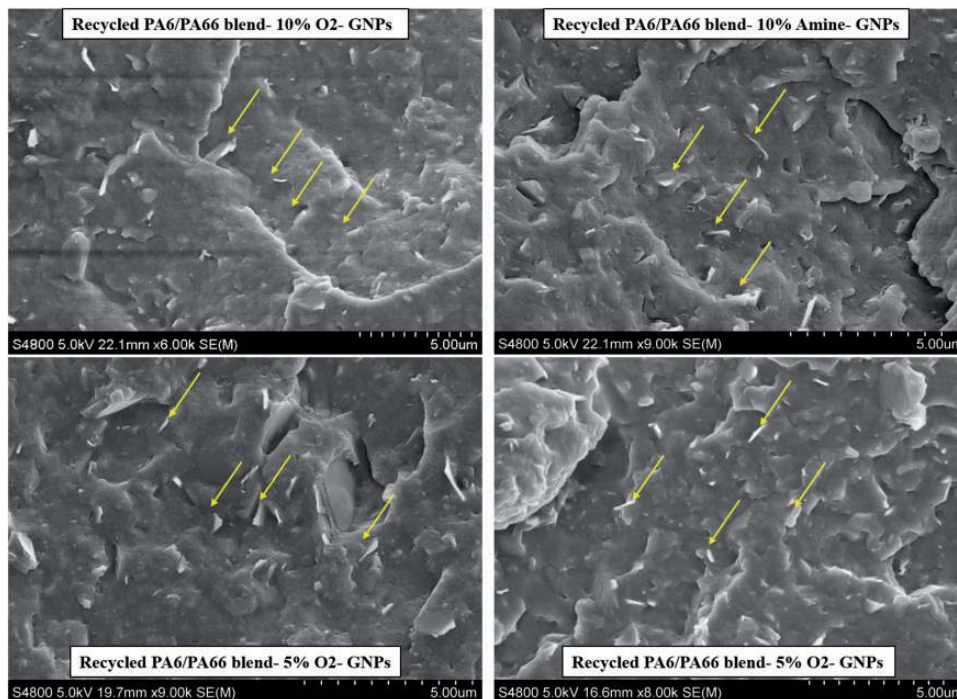


Figure 14. SEM images of the dispersion of both types of GNPs in the recycled nylons blend.

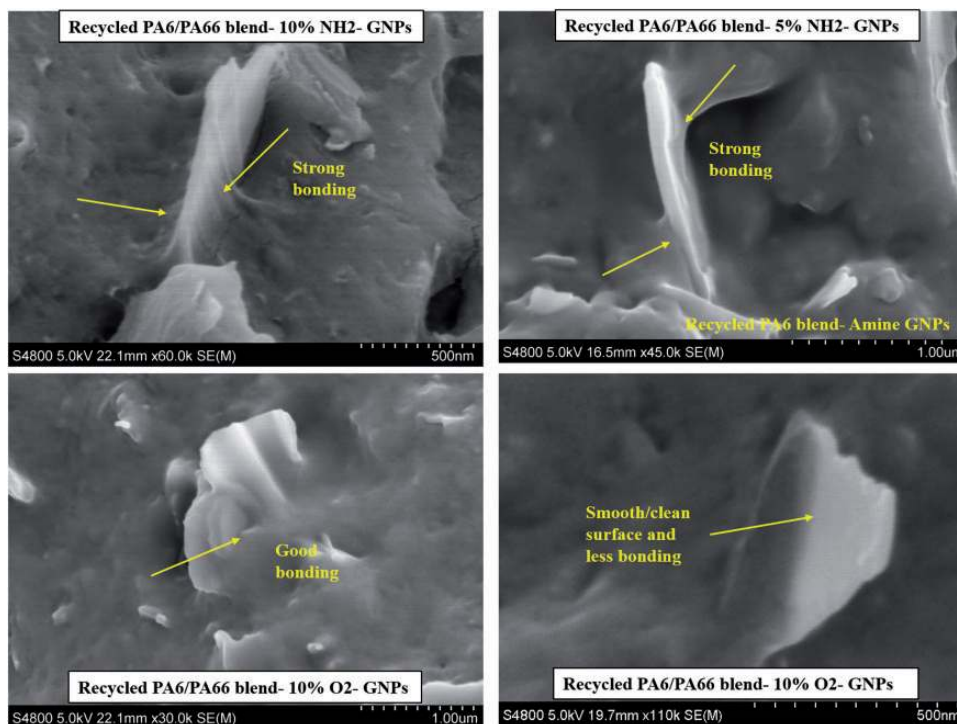


Figure 15. SEM images of the bonding of both types of GNPs to recycled nylons blend.

interfacial bonding between the recycled nylon blend and Amine-GNPs, while the bonding between the polymer and O₂-GNPs is not as strong and efficient since smooth and clean surface GNPs were spotted in some

areas. It can be concluded that functionalisation is crucial in obtaining carbon nanoparticles that are well distributed in the polymer matrix and strongly bonded to the host polymer chains. The improvements in

mechanical and thermal properties obtained in this study were attributed to the good dispersion of the nanoparticles and the strong interfacial interaction achieved between the nanoparticles and the recycled PA6/PA6,6 blend. The uniform distribution and good interfacial bonding and their effects on the properties of PAs and other polymers were also reported by other researchers.^{47,56,58–60}

Conclusion

Two types of functionalised GNPs (O_2 and NH_2) with a $500\text{ m}^2/\text{g}$ surface area were incorporated into recycled PA6/PA6,6 blends in order to enhance their mechanical and thermal properties. The overall crystallinity of the recycled nylon blend was not affected significantly. The effect of both functionalised GNPs on the thermal conductivity was significant. Both types of GNPs functionalisation led to notable increase in the thermal conductivity of the recycled PA6/PA6,6 blend with increasing both GNPs content. Amine-GNPs increased thermal conductivity by 59% compared to 26% increase with O_2 -GNPs at 10% GNP content. Shore hardness of the recycled nylon blend was also noticed to increase with increasing the content of both types of GNPs. Amine-GNPs again showed higher values of shore D hardness. Tensile and flexural stiffness of recycled PA6/PA6,6 blend improved by 102% with increasing the content of Amine-GNPs up to 10%. On the other hand, O_2 -GNPs reduced the tensile and flexural stiffness initially, but increase were evident at 10% GNPs. The Amine-GNPs was once more superior to O_2 -GNPs and provided higher modulus results. Tensile and flexural strength of the recycled PA6/PA6,6 blend were gradually increased with increasing of both GNPs content up to 2% followed by a reduction at higher GNPs concentrations. The tensile and flexural strength increased by 24% and 11% at 2% Amine-GNPs and O_2 -GNPs concentration, respectively. The degree of ductility was reduced with both types of functionalisation as the GNPs percentage increased. It can be concluded that 2% content of both Amine- and O_2 -graphene produced improvement in strength and stiffness without significantly affecting the ductility of the recycled nylon blend. Amine-GNPs have been more effective, which can be attributed to the chemical compatibility between the Amine group and nylon.

From the evidence in this study and microscopy images, it is reasonable to ascertain that the melt compounding resulted in an excellent dispersion of GNPs in the polymer matrix. It can also be said that the nanocomposite properties can be influenced by the dispersion and interfacial (Hydrogen) bonding between graphene and polymer. It would also be reasonable to state that the dispersion and bonding is influenced by

functional groups and particle size. The improvements in the properties of recycled PA6/PA6,6 blend obtained in this study by using functionalised graphene may open the door to industrial manufacturing of economical novel materials with excellent thermal conductivity, and mechanical performance.

Declaration of Conflicting Interests

The author(s) declared no potential conflicts of interest with respect to the research, authorship, and/or publication of this article.

Funding

The author(s) disclosed receipt of the following financial support for the research, authorship, and/or publication of this article: This work was supported by research fund of Ser Cymru National Research Network ('NRN') [7th Call-Industrial Collaboration Awards (ICA)] and Perpetuus Carbon Technology, Wales, UK.

ORCID iD

Feras Korkees  <https://orcid.org/0000-0002-5131-6027>

References

1. Subramanian MN. *Basics of polymers: Fabrication and processing technology*. New York: Momentum Press, 2015.
2. Darshan K, Naveen K, Rasmi H, et al. Mechanical and thermal behaviour of a recycle polypropylene using fillers as an additives. *Int J Sci Eng Technol Res* 2014; 3: 2532–2535.
3. Idowu I and Adekoya L. *Effects of filler on some mechanical properties of recycled low-density polyethylene composites*. Ile-Ife: Obafemi Awolowo University, Ile-Ife, 2015.
4. La Manila F. Effect of fillers on the properties of recycled polymers. *Macromol Symp* 2003; 194: 101–110.
5. Hill ME. Adding value to recycled polyethylene through the addition of multi-scale reinforcements. Thesis, The University of Akron, USA, 2005.
6. Pelin CE, Ficai A, Andronescu E, et al. Recycling and reusing polyamide 6 extruded waste products to manufacture carbon fiber based composites. *Annals of the Academy of Romanian Scientists Series on Physics and Chemistry Science* 2017; 2: 91–103.
7. Wesolowski J and Plachta K. The polyamide market. *Fibres Text East Eur* 2016; 24: 12–18.
8. Grand View Research. Nylon 6 & 66 Market Analysis By Product (Nylon 6, Nylon 66) By Application (Automotive, Electrical & Electronic, Engineering Plastic, Textiles, Others), By Region, And Segment Forecasts, 2018. – 2025. Available at: <https://www.grandviewresearch.com/industry-analysis/nylon-6-6-market> (2020, accessed 10 September 2020).
9. Li N, Mahat D and Park A. Reduce, reuse, and replace: a study on solutions to plastic wastes. An Interactive Qualifying Project Submitted to the faculty of Worcester Polytechnic Institute, 2009.

10. MarketsandMarkets. Polyamide Market by Application (Engineering Plastics, Fiber), Type (PA 6, PA 66, Bio-based & Specialty Polyamides), and Region (Asia-Pacific, North America, Europe, Middle East & Africa, South America) – Global forecast to 2021. Available at: <https://www.marketsandmarkets.com/Market-Reports/global-nylon-market-930.html> (2020, accessed 10 September 2020).
11. Lambert S. Environmental risk of polymers and their degradation products. Thesis, University of York, USA, 2013.
12. Weckstrom D. Changes in mechanical properties of recycled polypropylene. *Degree Thesis*, Arcada-University of Applied Science, Finland, 2012.
13. Li A, Zhang C and Zhang Y. Thermal conductivity of graphene-polymer composites: mechanisms, properties, and applications. *Polymers* 2017; 9: 437.
14. Strobl G. *The physics of polymers*. Berlin: Springer-Verlag Berlin Heidelberg, 2007.
15. Ali H. Introduction to Polymer Blend lecture 1. Lecture presented at College of Materials Engineering, University of Babylon, Iraq, 2016.
16. Karger-Kocsis J. *Polypropylene-polymer blend*. 2nd ed. Dordrecht: Springer, 1999.
17. Oshinski A, Keskkula H and Paul D. Rubber toughening of polyamides with functionalized block copolymers: 1. Nylon-6. *Polymer* 1992; 33: 268–283.
18. Rybníkář F and Geil PH. Melting and recrystallization of PA-6/PA-66 blends. *J Appl Polym Sci* 1993; 49: 1175–1188.
19. Takeda Y, Keskkula H and Paul D. Effect of polyamide functionality on the morphology and toughness of blends with a functionalized block copolymer. *Polymer* 1992; 33: 3173–3181.
20. Matweb. PA6/PA66 blend properties. Available at: <http://www.matweb.com/search/DataSheet.aspx?MatGUID=e1c29525c42f45aea3899f5d225f5f01&ckck=1> (2020, accessed 10 September 2020).
21. Chen J, Wu W, Chen C, et al. Toughened nylon66/nylon6 ternary nanocomposites by elastomers. *J Appl Polym Sci* 2010; 115: 588–598.
22. Bose S, Bhattacharyya A, Kulkarni A, et al. Electrical, rheological and morphological studies in co-continuous blends of polyamide 6 and acrylonitrile-butadiene-styrene with multiwall carbon nanotubes prepared by melt blending. *Compos Sci Technol* 2009; 69: 365–372.
23. Xiao C, Leng X, Zhang X, et al. Improved thermal properties by controlling selective distribution of AlN and MWCNT in immiscible polycarbonate (PC)/polyamide 66 (PA66) composites. *Compos Part A: Appl Sci Manuf* 2018; 110: 133–141.
24. Kusmono Mohd Ishak Z, Chow W, Takeichi T, et al. Compatibilizing effect of SEBS-g-MA on the mechanical properties of different types of OMMT filled polyamide 6/polypropylene nanocomposites. *Compos Part A: Appl Sci Manuf* 2008; 39: 1802–1814.
25. Yuan D, Gao Y, Guo Z, et al. Improved thermal conductivity of ceramic filler-filled polyamide composites by using PA6/PA66 1:1 blend as matrix. *J Appl Polym Sci* 2017; 134: 45371.
26. Arboleda-Clemente L, Ares-Pernas A, García X, et al. Influence of polyamide ratio on the CNT dispersion in polyamide 66/6 blends by dilution of PA66 or PA6-MWCNT masterbatches. *Synth Metals* 2016; 221: 134–141.
27. Arboleda-Clemente L, García-Fonte X, Abad M, et al. Role of rheology in tuning thermal conductivity of polyamide 12/polyamide 6 composites with a segregated multiwalled carbon nanotube network. *J Compos Mater* 2018; 52: 2549–2557.
28. Chow W and Mohd Ishak Z. Polyamide blend-based nanocomposites: a review. *Express Polym Lett* 2015; 9: 211–232.
29. Ferreira C, Perez C, Hirayama D, et al. Recycling of polyamide (PA) from scrap tires as composites and blends. *J Environ Chem Eng* 2013; 1: 762–767.
30. Faruk O, Kc B, Tjong J, et al. Automotive prototype from recycled carbon fiber reinforced recycled polyamide composite. In: *ANTEC Toronto: Center for biocomposites and biomaterials processing*. Canada: University of Toronto, 2017. pp. 275–279.
31. Medeiros D, Jardim P, de Tatagiba M, et al. Composites of recycled nylon 11 and titanium based nanofillers. *Polym Test* 2015; 42: 108–114.
32. Gardner DJ and Han Y. *Mechanical properties of hybrid basalt-carbon fiber-filled recycled polypropylene and polyamide 6 composites*. Maine: University of Maine, 2017.
33. Szustakiewicz K, Gazińska M, Kiersnowski A, et al. Polyamide 6/organomontmorillonite nanocomposites based on waste materials. *Polimery-Warsaw* 2011; 56: 397–400.
34. Zare Y. Recent progress on preparation and properties of nanocomposites from recycled polymers: a review. *Waste Manage* 2013; 33: 598–604.
35. Mayoral B, Harkin-Jones E, Khanam PN, et al. Melt processing and characterisation of polyamide 6/graphene nanoplatelet composites. *RSC Adv* 2015; 5: 52395–52409.
36. Mindivan F. Effect of graphene nanoplatelets (GNPs) on tribological and mechanical behaviors of polyamide 6 (PA6). *Tribol Ind* 2017; 39: 277–282.
37. Yu A. Carbon nanotubes and graphene nanoplatelets for multi-functional composites. University of Waterloo. Available at: <https://uwaterloo.ca/institute-polymer-research/sites/ca.institute-polymer-research/files/uploads/files/aipingyu.pdf> (2010, accessed 10 September 2020).
38. Zhou S, Yu L, Song X, et al. Preparation of highly thermally conducting polyamide 6/graphite composites via low-temperature in situ expansion. *J Appl Polym Sci* 2014; 131.
39. Cai D and Song M. A simple route to enhance the interface between graphite oxide nanoplatelets and a semi-crystalline polymer for stress transfer. *Nanotechnology* 2009; 20: 315708.
40. Arboleda L, Ares A, Abad M, et al. Piezoresistive response of carbon nanotubes-polyamides composites processed by extrusion. *J Polym Res* 2013; 20: 326.

41. Wang Y, Zhan HF, Xiang Y, et al. Effect of covalent functionalization on thermal transport across graphene–polymer interfaces. *J Phys Chem C* 2015; 119: 12731–12738.
42. Ha S, Kwon O, Oh Y, et al. Thermally conductive polyamide 6/carbon filler composites based on a hybrid filler system. *Sci Technol Adv Mater* 2015; 16: 065001.
43. Song N, Yang J, Ding P, et al. Effect of polymer modifier chain length on thermal conductive property of polyamide 6/graphene nanocomposites. *Compos Part A: Appl Sci Manuf* 2015; 73: 232–241.
44. Noorunnisa Khanam P, Al Maadeed M, Ouederni M, et al. Effect of two types of graphene nanoplatelets on the physico–mechanical properties of linear low–density polyethylene composites. *Adv Manuf Polym Compos Sci* 2016; 2: 67–73.
45. Xu B, Lin Z, Du C, et al. Mechanical properties, morphology and thermal conductivity of polyamide composites filled with graphene nanoplatelets, Al₂O₃ and graphite. *Mater Res Innov* 2015; 19: S1-388–S1-391.
46. Chen Y, Gao J, Yan Q, et al. Advances in graphene-based polymer composites with high thermal conductivity. *Veruscript Funct Nanomater* 2018; 2: 1–17.
47. Satheeskumar S and Kanagaraj G. Experimental investigation on tribological behaviours of PA6, PA6-reinforced Al₂O₃ and PA6-reinforced graphite polymer composites. *Bull Mater Sci* 2016; 39: 1467–1481.
48. Onyu K, Yeetsorn R, Fowler M, et al. Evaluation of the possibility for using polypropylene/graphene composite as bipolar plate material instead of polypropylene/graphite composite. *KMUTNB Int J Appl Sci Technol* 2016; 9: 1–13.
49. Ando M, Kalacska G and Czigany T. Shore D hardness of cast PA6 based composites. *Sci Bull Ser C: Fascicle Mech* 2009; 23: 15–18.
50. La D, Nguyen T, Quoc V, et al. A new approach of fabricating graphene nanoplates@natural rubber latex composite and its characteristics and mechanical properties. *J Carbon Res* 2018; 4(3): 50.
51. Mindivan F. Effect of Graphene Nanoplatelets (GNPs) on Tribological and Mechanical Behaviors of Polyamide 6 (PA6). *Tribology in Industry* 2017; 39: 277–282.
52. Yesildag N, Hopmann C, Adamy M, et al. Properties of polyamide 6-graphene-composites produced and processed on industrial scale. In: *AIP Conference Proceedings 1914*, 2017. AIP Publishing LLC. DOI: 10.1063/1.5016778.
53. Halit M. Processing, structure and properties of polyamide 6/graphene nanoplatelets nanocomposites. Thesis, University of Manchester, UK, 2018.
54. Keledi G, Hári J and Pukánszky B. Polymer nanocomposites: structure, interaction, and functionality. *Nanoscale* 2012; 4: 1919–1938.
55. Umar M. Processing, structure and properties of PA6/carbon composites. Thesis, University of Manchester, UK, 2014.
56. Liu W, Do I, Fukushima H, et al. Influence of processing on morphology, electrical conductivity and flexural properties of exfoliated graphite nanoplatelets-polyamide nanocomposites. *Carbon Lett* 2010; 11: 279–284.
57. Ma Y, Zhou T, Su G, et al. Understanding the crystallization behavior of polyamide 6/polyamide 66 alloys from the perspective of hydrogen bonds: projection moving-window 2D correlation FTIR spectroscopy and the enthalpy. *RSC Adv* 2016; 6: 87405–87415.
58. Li J, Gunister E and Barsoum I. Effect of graphene oxide as a filler material on the mechanical properties of LLDPE nanocomposites. *J Compos Mater* 2019; 53: 2761–2773.
59. Vadukumpully S, Paul J, Mahanta N, et al. Flexible conductive graphene/poly(vinyl chloride) composite thin films with high mechanical strength and thermal stability. *Carbon* 2011; 49: 198–205.
60. Wang F, Drzal L, Qin Y, et al. Mechanical properties and thermal conductivity of graphene nanoplatelet/epoxy composites. *J Mater Sci* 2015; 50: 1082–1093.